



Photocatalytic oxidation of the organic monolayers on TiO₂ surface investigated by in-situ sum frequency generation spectroscopy

Yujin Tong, Qiling Peng, Tongsen Ma, Takuma Nishida, and Shen Ye

Citation: *APL Materials* **3**, 104402 (2015); doi: 10.1063/1.4921954

View online: <http://dx.doi.org/10.1063/1.4921954>

View Table of Contents: <http://scitation.aip.org/content/aip/journal/aplmater/3/10?ver=pdfcov>

Published by the [AIP Publishing](#)

Articles you may be interested in

[Photocatalytic and antibacterial properties of Au-TiO₂ nanocomposite on monolayer graphene: From experiment to theory](#)

J. Appl. Phys. **114**, 204701 (2013); 10.1063/1.4836875

[Efficiently recyclable magnetic core-shell photocatalyst for photocatalytic oxidation of chlorophenol in water](#)

J. Appl. Phys. **111**, 07B504 (2012); 10.1063/1.3671782

[A theoretical investigation on photocatalytic oxidation on the TiO₂ surface](#)

J. Chem. Phys. **136**, 024706 (2012); 10.1063/1.3676261

[Chemical imaging of interfaces by sum-frequency generation microscopy: Application to patterned self-assembled monolayers](#)

Appl. Phys. Lett. **83**, 3830 (2003); 10.1063/1.1624465

[Chain-length-dependent change in the structure of self-assembled monolayers of n-alkanethiols on Au\(111\) probed by broad-bandwidth sum frequency generation spectroscopy](#)

J. Chem. Phys. **118**, 1904 (2003); 10.1063/1.1531098

Launching in 2016!
The future of applied photonics research is here

Photocatalytic oxidation of the organic monolayers on TiO₂ surface investigated by *in-situ* sum frequency generation spectroscopy

Yujin Tong,^a Qiling Peng, Tongsen Ma,^b Takuma Nishida, and Shen Ye^c

Catalysis Research Center, Hokkaido University, Sapporo 060-0811, Japan

(Received 26 April 2015; accepted 20 May 2015; published online 1 June 2015)

In-situ vibrational sum frequency generation (SFG) spectroscopy has been employed to investigate the photocatalytic oxidation of two types of well-ordered organic monolayers, namely, an arachidic acid (AA) monolayer prepared by the Langmuir-Blodgett method and an octadecyltrichlorosilane (OTS) monolayer prepared by the self-assembling method, on a TiO₂ surface under ultraviolet (UV) irradiation. The extremely high sensitivity and unique selectivity of the SFG spectroscopy enabled us to directly probe the structural changes in these monolayers during the surface photocatalytic oxidation and further elucidate their reaction mechanisms at a molecular level. It was revealed that the ordering of the monolayers during the photocatalytic reaction is strongly dependent on their interaction with the substrate; the AA monolayer maintains its ordered conformation until the final oxidation stage, while the OTS monolayer shows a large increase in disordering during the initial oxidation stage, indicating a different photocatalytic reaction mechanism of the two monolayers on the TiO₂ surface. © 2015 Author(s). All article content, except where otherwise noted, is licensed under a Creative Commons Attribution 3.0 Unported License. [<http://dx.doi.org/10.1063/1.4921954>]

Titanium dioxide (TiO₂) has versatile applications from dye sensitized solar cell to surface coating and has attracted much interest as a photocatalyst due to its high activity and stability.¹⁻⁴ It was reported that small organic molecules can be photocatalytically oxidized on the TiO₂ surface under ultraviolet (UV) irradiation. The photocatalytic reaction is now widely applied in the field of environmental protection, such as environmental decontamination and self-cleaning.¹⁻³ While most of the previous studies focused on small volatile molecules, there were only a very few studies on the photocatalytic reaction of long-chain organic molecules in a monolayer with well-defined structure.⁵⁻⁸ As a model system for the photocatalytic reaction, the monolayers of long-chain organic molecules are both of practical and fundamental interests.⁹ Understanding the photo-induced oxidation mechanism of organic thin-films is crucial for developing novel functional materials for environmental protection. Although the mechanism for the photocatalytic oxidations on the TiO₂ has been extensively investigated,¹⁻⁴ our knowledge about the photocatalytic oxidation of such monolayers on the TiO₂ surface is still limited at a molecular level. For example, how does the molecular structure of the monolayer change during the reaction? How does the interaction between the organic molecule and TiO₂ surface affect the reaction kinetics?

In the present study, by employing vibrational sum frequency generation (SFG) spectroscopy, the structural changes in the well-ordered monolayers of organic molecules with long alkyl chain on the TiO₂ surface under UV irradiation were investigated at a molecular level. Vibrational SFG is a 2nd-order non-linear optical technique and has been employed to probe molecule structures on various surfaces and interfaces.¹⁰⁻²⁰ In addition to its high surface sensitivity, SFG spectroscopy

^aPresent address: Fritz Haber Institute of the Max Planck Society, 14195 Berlin, Germany.

^bPresent address: Department of Chemistry, Henan University, China.

^cAuthor to whom correspondence should be addressed. Electronic mail: ye@cat.hokudai.ac.jp.



shows a very unique response to the symmetry and ordering of the molecules, providing significant information about the molecular structures in comparison to conventional vibrational spectroscopy.^{21–25} In the present study, we revealed the different oxidation behaviors of two types of well-ordered monolayers, namely, the Langmuir-Blodgett (LB) monolayer and self-assembling monolayer (SAM) of organic molecules with long alkyl chains,^{26–28} and demonstrated how the interaction between the organic molecules and substrate affects the oxidation behaviors. This study provides a molecular level understanding regarding the photocatalytic reaction mechanism on the TiO₂ surface.

The polycrystalline TiO₂ (anatase) films were obtained by a sol-gel method.²⁹ The diluted titanium tetraisopropoxide solution (NDH-510C, Nippon Soda) was spin-coated on the flat surface of a hemicylindrical fused quartz surface at 2000 rpm and then sintered at 500 °C for 30 min in air. This procedure produced a TiO₂ film with its thickness of 120 nm having a surface roughness of ca. 1.3 nm.²⁹ A LB monolayer of arachidic acid (AA), CH₃(CH₂)₁₈COOH (AA), was constructed on the surface of water containing 0.3 mM NaHCO₃ and 0.2 mM CdCl₂ (pH = 6.6) in a LB trough (FSD-500, USI) at room temperature and then transferred to the substrate surface at a surface pressure of 30 mN/m.^{30,31} A SAM of octadecyltrichlorosilane (OTS) was prepared on the TiO₂ surface following the procedures described elsewhere.^{32–36}

A broad-band SFG system was used to characterize the structure and conformational ordering of the two monolayers. Details about the system were described elsewhere.^{37,38} A broad-band femtosecond infrared pulse of 3 μJ (FWHM ~200 cm⁻¹, centered at 2900 cm⁻¹) and a narrow-band picosecond visible pulse of 8 μJ at 800 nm (FWHM ~10 cm⁻¹) were spatially and temporally overlapped at the sample surface with incident angles of 50° and 65°, respectively. An SFG signal was detected by a CCD detector attached to the spectrograph. The time-resolved SFG spectra were recorded with the *ppp* (*p*-polarized SFG, *p*-visible, and *p*-IR) polarization combination and acquisition time of 10 s/spectrum. All the SFG spectra were normalized by a vibrationally non-resonant SFG signal from a gold thin-film (200 nm in thickness) deposited on the flat surface of a fused quartz prism with identical shape as those used for TiO₂ coating. A “black light” lamp with a 365 nm maximum (Toshiba FL4BLB) was used as the UV irradiation source. The UV irradiation intensity at the sample surface was ca. 5 mW/cm². The surface hydrophobicity was also evaluated by the contact angle measurement.

Figure 1(a) shows the time-resolved *ppp*-polarized SFG spectra (2800–3000 cm⁻¹) of the LB monolayer of AA on the TiO₂ surface under UV irradiation. Before the UV-irradiation, three major SFG peaks were observed at 2878, 2938, and 2967 cm⁻¹. These peaks can be assigned to the C–H symmetric, Fermi resonance between the C–H symmetric and overtone of C–H bending, and C–H asymmetric stretching of the terminal CH₃ group of AA molecules in the monolayer, respectively. The two shoulders at 2848 and 2920 cm⁻¹ were attributed to the C–H symmetric and asymmetric

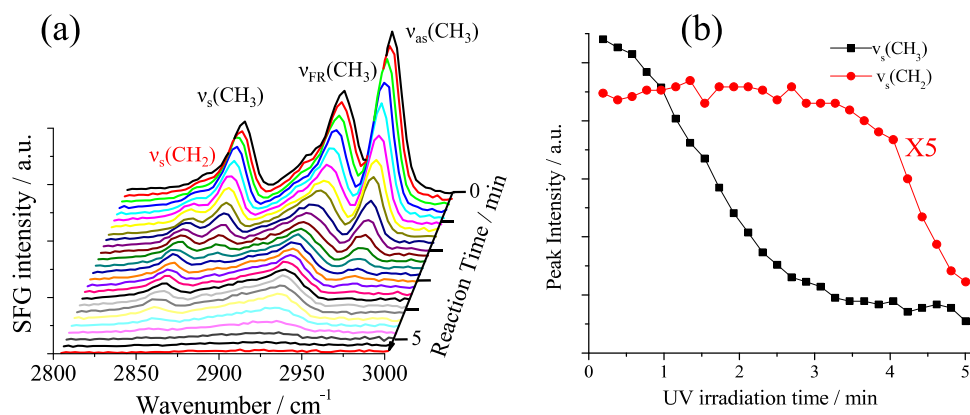


FIG. 1. (a) Time-resolved *ppp*-polarized SFG spectra in C–H stretching region of LB-monolayer of AA molecules on TiO₂ surface as a function of UV irradiation time (0–5 min). (b) SFG intensity of CH₃ (black squares) and CH₂ mode (red circles) as a function of UV irradiation time. Solid lines are only for visual guide.

modes of the CH₂ group in the long alkyl chain of AA, respectively.^{30,31} As already discussed, the vibration modes of the CH₂ group in a long alkyl chain with an *all-trans* conformation are SFG-inactive due to the centrosymmetric structure; thus, the SFG peaks observed for the CH₂ group cannot be used to evaluate its population but mainly used to characterize the number of the *gauche* defects in the long alkyl chains.^{39,40} The conformational *gauche* defects break the *all-trans* structure of the alkyl chain and reflect the disordering of the monolayer. Thus, the weak SFG intensity of CH₂ compared to that of CH₃ in Fig. 1(a) indicates that an *all-trans* conformation of the AA monolayer with only a very small amount of *gauche* defects was constructed.^{30,31} The contact angle measurements showed that the surface is very hydrophobic (>90°). As soon as the UV irradiation started, the SFG spectra quickly changed. Figure 1(b) shows the peak intensities for the symmetric stretching modes of the CH₃ and CH₂ groups as a function of the UV-irradiation time. The peak intensity for the CH₃ group dramatically decreased and reached ca. 15% of its initial value within 2 min, then further reduced to a background level after 3 min. In contrast, the peak intensity of the CH₂ group was nearly constant during the initial period and started to decrease as the CH₃ peak was almost negligible and finally disappeared after 5 min (Fig. 1), and the surface became completely hydrophilic. As a control experiment, no change in the SFG signal and contact angle was observed for the AA monolayer deposited on a fused quartz surface under the UV-irradiation. The decay behaviors of the two peaks are considered to be a result of the photocatalytic oxidation of the AA monolayer on the TiO₂ surface under UV-irradiation.

Since the SFG intensity is proportional to the square of the population of the related species on the surface, the oxidation kinetics of the terminal CH₃ group in the monolayer can be determined from the decay profile (Fig. 1(b)). However, since the surface density of the CH₃ group is not necessarily the same as the coverage of the partially oxidized monolayer during the photocatalytic reaction, the time-dependent SFG intensity of the CH₃ group (Fig. 1(b)) is no longer a suitable probe for the monolayer coverage. Thereby, we could not use the ratio between the peak amplitude of CH₂ and CH₃ groups to specify the ordering of the film as typically done by previous studies.^{37,38,41,42} Instead, we could employ the number of the *gauche* defects, i.e., the peak amplitude of the CH₂ group, to characterize the relative ordering of the film during the photocatalytic oxidation reaction. Based on the assumption, the AA monolayer seems to maintain the same ordering during the first stage of the oxidation. As the terminal CH₃ groups were almost oxidatively decomposed, the relative disordering started to decrease, implying that a very specific ordering change occurs during the photocatalytic reaction for the AA monolayer on the TiO₂ surface.

Figure 2(a) shows the time-resolved SFG spectra for SAM of the OTS monolayer on the TiO₂ surface under the UV-irradiation. Before the UV-irradiation, the SFG spectrum for the OTS monolayer was very similar to those of the AA monolayer, i.e., three major peaks attributed to the

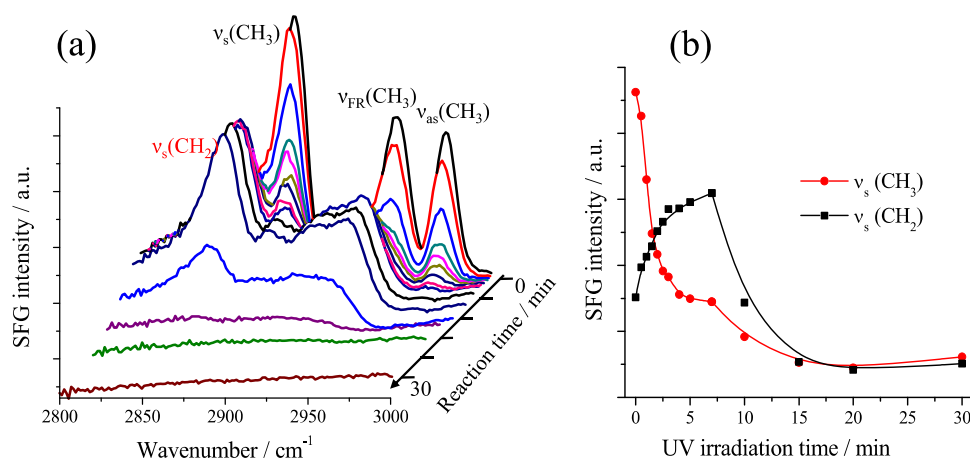
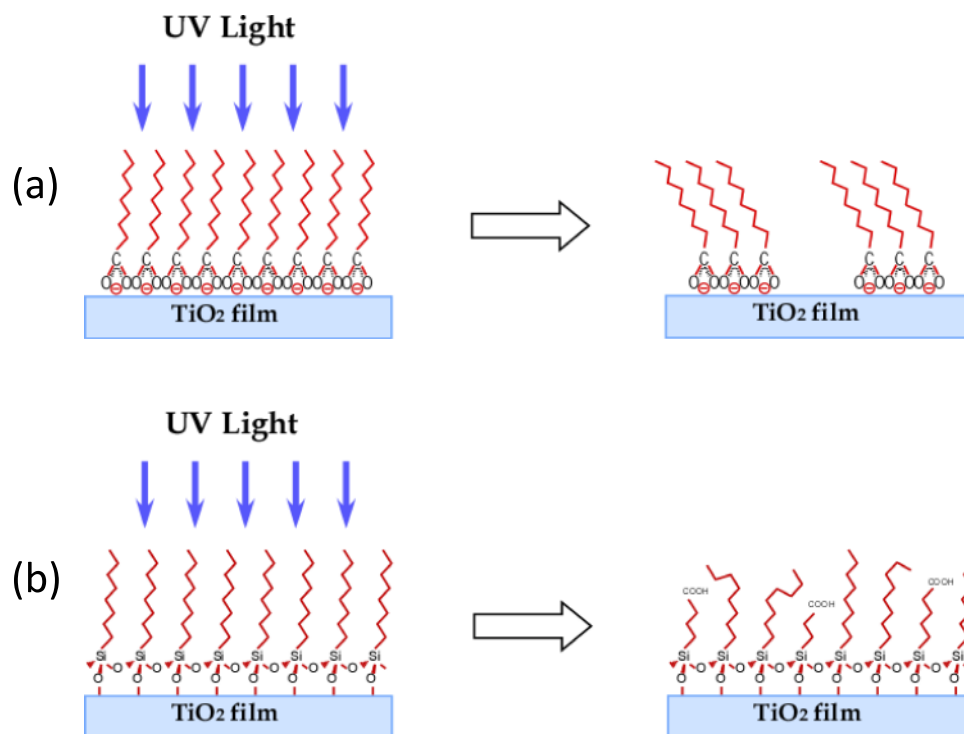


FIG. 2. (a) Time-resolved *ppp*-polarized SFG spectra in C–H stretching region of SAM of OTS on TiO₂ surface as a function of UV irradiation time. (b) SFG intensity of CH₃ (black squares) and CH₂ mode (red circles) as a function of UV irradiation time. Solid lines are only for visual guide.

CH₃ group were mainly observed with small shoulders for the CH₂ group. This indicated that a well-defined SAM of the OTS was constructed on the TiO₂ surface. The SFG spectra of the OTS monolayer under the UV-irradiation show quite different features in comparison to the AA monolayer (Fig. 1). The SFG intensity of the CH₃ group decreased while that of the CH₂ group initially increased (0–7 min) and then decreased (Fig. 2(b)). In the first stage, the SFG intensities for the CH₃ and CH₂ exhibited totally opposite changes with the UV-irradiation and reached a somewhat saturated value at the end of the stage. In the next stage (7 min), the SFG intensity for the CH₂ group then decreased and dropped to a background level in 10 min, while the decrease of the CH₃ intensity slowed down and disappeared at the same time (Fig. 2(b)).

In comparison to the AA monolayer on the TiO₂ surface, a longer time is needed to fully oxidize the OTS monolayer on the TiO₂ surface under the UV-irradiation. Furthermore, it is interesting to notice that the SFG intensity for the CH₂ group in the OTS monolayer largely increased during the first stage and decreased in the second stage, which reflects changes of the number of *gauche* defects during the two stages. Based on the same assumption mentioned above, this implies that the OTS monolayer suffers significant order to disorder change during the first oxidation stage, while the disordering seems to decrease in the second stage.

To explain the different photocatalytic oxidation features observed in Figs. 1 and 2, a reaction scheme is proposed (Scheme 1). Since the AA monolayer was transferred from the water subphase to the TiO₂ surface at a surface pressure of 30 mN/m by the LB method, the AA molecules in the monolayer are expected to take a solid-like structure based on the features of the π -A isotherm.^{26–28} This structure has also been confirmed by the SFG spectrum before the UV-irradiation. Furthermore, a very thin layer of water is known to be formed between the organic monolayer and hydrophilic substrate surface during the transfer process.^{37,38} On the other hand, it is known from previous studies that the long-chain fatty acid molecules tend to aggregate together to form condensed domains where an attractive van der Waals interaction works between the AA molecules on the water surface.^{26–28} We believe that a similar process also occurs for the AA monolayer on the hydrophilic TiO₂ surface during the UV-irradiation. Since there are no covalent bond between the AA's polar



SCHEME 1. Schematic model for photocatalytic oxidation reaction for (a) physisorbed AA monolayer and (b) chemisorbed OTS monolayer on TiO₂ surface during UV irradiation.

headgroup and the TiO₂ substrate, AA molecules can have a higher mobility on the TiO₂ surface due to the presence of the thin water layer between the AA monolayer and substrate. When some of the AA molecules in the monolayer are oxidized by the UV-irradiation, the surrounded AA molecules can diffuse and reconstruct to form the condensed domains by the intermolecular van der Waals interaction. These condensed domains have a conformational ordering similar to those in the monolayer before the UV-irradiation (Scheme 1(a)), and even the total coverage for the AA monolayer becomes very low. On the other hand, in the case of OTS monolayer, hydrolyzed OTS molecules are anchored not only on the TiO₂ surface with the Si–O bond but also bind to each other by the Si–O–Si network through the silane coupling reaction.^{32,33} The strong chemical interaction in the OTS monolayer restricts the lateral mobility of the individual OTS molecule in the monolayer. When some of the OTS molecules in the SAM were oxidized, the remaining OTS molecules could not repair the oxidized sites (Scheme 1(b)) in order to reconstruct ordered domains by a surface diffusion process as that happen on the AA monolayer. This is considered as the main reason that the *gauche* defects continuously increase during the first stage of the photocatalytic oxidation of the OTS monolayer (Fig. 2(b)). The number of *gauche* defects in the OTS monolayer decreased with the full oxidative decomposition of the monolayer (Scheme 1(b)). The contact angle measurements showed that the TiO₂ surface changed from hydrophobic to hydrophilic after the UV-irradiation. The present SFG measurements were only carried out in the C–H stretching region. Further SFG measurements in lower frequency regions for possible reaction products and intermediates such as carboxylate and carboxylic acid groups are still in progress in our group.

The present photocatalytic oxidation mechanism (Scheme 1) is in agreement with previous morphological observations by atomic force microscopy (AFM). Fujishima and Hashimoto investigated the UV-induced oxidation of the LB-multilayer of stearic acid on the TiO₂ surface and reported that many island domain structures were formed during the photocatalytic decomposition process.⁵ This indicates that the unoxidized fatty acid molecules are reconstructed to form stable domains on the TiO₂ surface during the photocatalytic process. In contrast, Lee *et al.* studied the UV-induced decomposition of the OTS monolayer on the TiO₂ surface and demonstrated that a homogeneous reduction of the film thickness, implying that the immobilized OTS molecules were oxidized from the terminal CH₃ group to the other end of the molecule without formation of the ordered domains during the oxidation process.⁷

In the present study, vibrational SFG spectroscopy was employed to study the UV-induced photocatalytic oxidation of two types of well-ordered monolayers on the TiO₂ surface. By monitoring the ordering of the monolayers during the photocatalytic oxidation, we could reveal the different reaction mechanisms for these monolayers; namely, a physisorbed AA monolayer maintains its ordered structure through the lateral diffusion, and a chemisorbed monolayer becomes more disordered during the reaction due to the limited mobility on the substrate surface. This study provides essential information for understanding the photocatalytic decomposition of organics with long alkyl chains on the TiO₂ surfaces and is intimately related to application of the TiO₂ as a photocatalyst and photoactive material for antifouling, antibacterial, and self-cleaning.

This work was supported by a Grant-in-Aid for Scientific Research on Innovative Areas “Coordination Program” 759 (24108701) and a Grant-in-Aid for Scientific Research (B) 23350058 from the Ministry of Education, Culture, Sports, Science and Technology (MEXT), Japan.

¹ A. Fujishima, X. Zhang, and D. A. Tryk, *Surf. Sci. Rep.* **63**, 515 (2008).

² M. A. Henderson, *Surf. Sci. Rep.* **66**, 185 (2011).

³ T. L. Thompson and J. T. Yates, *Chem. Rev.* **106**, 4428 (2006).

⁴ A. Hagfeldt, G. Boschloo, L. Sun, L. Kloo, and H. Pettersson, *Chem. Rev.* **110**, 6595 (2010).

⁵ P. Sawunyama, L. Jiang, A. Fujishima, and K. Hashimoto, *J. Phys. Chem. B* **101**, 11000 (1997).

⁶ E. Balaur, J. M. Macak, L. Taveira, and P. Schmuki, *Electrochem. Commun.* **7**, 1066 (2005).

⁷ J. P. Lee, H. K. Kim, C. R. Park, G. Park, H. T. Kwak, S. M. Koo, and M. M. Sung, *J. Phys. Chem. B* **107**, 8997 (2003).

⁸ A. Mills and M. McFarlane, *Catal. Today* **129**, 22 (2007).

⁹ T. Minabe, D. A. Tryk, P. Sawunyama, Y. Kikuchi, K. Hashimoto, and A. Fujishima, *J. Photochem. Photobiol., A* **137**, 53 (2000).

¹⁰ Y. R. Shen, *The Principles of Nonlinear Optics* (John Wiley & Sons, Inc., New York, 1984).

¹¹ C. D. Bain, *J. Chem. Soc., Faraday Trans.* **91**, 1281 (1995).

¹² P. Miranda and Y. R. Shen, *J. Phys. Chem. B* **103**, 3292 (1999).

¹³ Z. Chen, Y. R. Shen, and G. A. Somorjai, *Annu. Rev. Phys. Chem.* **53**, 437 (2002).

- ¹⁴ G. L. Richmond, *Chem. Rev.* **102**, 2693 (2002).
- ¹⁵ J. Holman, P. B. Davies, T. Nishida, S. Ye, and D. J. Neivandt, *J. Phys. Chem. B* **109**, 18723 (2005).
- ¹⁶ S. Ye and M. Osawa, *Chem. Lett.* **38**, 386 (2009).
- ¹⁷ Y. R. Shen, *Annu. Rev. Phys. Chem.* **64**, 129 (2013).
- ¹⁸ S. Nihonyanagi, J. A. Mondal, S. Yamaguchi, and T. Tahara, *Annu. Rev. Phys. Chem.* **64**, 579 (2013).
- ¹⁹ S. Ye, Y. Tong, A. Ge, L. Qiao, and P. B. Davies, *Chem. Rec.* **14**, 791 (2014).
- ²⁰ E. C. Y. Yan, L. Fu, Z. Wang, and W. Liu, *Chem. Rev.* **114**, 8471 (2014).
- ²¹ K. Uosaki, T. Yano, and S. Nihonyanagi, *J. Phys. Chem. B* **108**, 19086 (2004).
- ²² C. Wang, H. Groenzin, and M. J. Shultz, *Langmuir* **19**, 7330 (2003).
- ²³ C. Wang, H. Groenzin, and M. J. Shultz, *J. Phys. Chem. B* **108**, 265 (2004).
- ²⁴ C. Wang, H. Groenzin, and M. J. Shultz, *J. Am. Chem. Soc.* **126**, 8094 (2004).
- ²⁵ S. Ye, A. Kathiravan, H. Hayashi, Y. Tong, Y. Infahsaeng, P. Chabera, T. Pascher, A. P. Yartsev, S. Isoda, H. Imahori, and V. Sundström, *J. Phys. Chem. C* **117**, 6066 (2013).
- ²⁶ A. Ulman, *Chem. Rev.* **96**, 1533 (1996).
- ²⁷ M. C. Petty, *Langmuir-Blodgett Films: An Introduction* (Cambridge University Press, Cambridge, 1996).
- ²⁸ A. Ulman, *An Introduction to Ultrathin Organic Films: From Langmuir-Blodgett to Self-Assembly* (Academic Press, San Diego, CA, 1991).
- ²⁹ N. Sakai, A. Fujishima, T. Watanabe, and K. Hashimoto, *J. Phys. Chem. B* **107**, 1028 (2003).
- ³⁰ S. Ye, H. Noda, S. Morita, K. Uosaki, and M. Osawa, *Langmuir* **19**, 2238 (2003).
- ³¹ S. Ye, H. Noda, T. Nishida, S. Morita, and M. Osawa, *Langmuir* **20**, 357 (2004).
- ³² J. Sagiv, *J. Am. Chem. Soc.* **102**, 92 (1980).
- ³³ S. Ye, S. Nihonyanagi, and K. Uosaki, *Phys. Chem. Chem. Phys.* **3**, 3463 (2001).
- ³⁴ Y. Tong, E. Tyrode, M. Osawa, N. Yoshida, T. Watanabe, A. Nakajima, and S. Ye, *Langmuir* **27**, 5420 (2011).
- ³⁵ S. Marcinko and A. Y. Fadeev, *Langmuir* **20**, 2270 (2004).
- ³⁶ R. Helmy and A. Y. Fadeev, *Langmuir* **18**, 8924 (2002).
- ³⁷ A. Ge, H. Wu, T. A. Darwish, M. James, M. Osawa, and S. Ye, *Langmuir* **29**, 5407 (2013).
- ³⁸ A. Ge, Q. Peng, H. Wu, H. Liu, Y. Tong, T. Nishida, N. Yoshida, K. Suzuki, T. Sakai, M. Osawa, and S. Ye, *Langmuir* **29**, 14411 (2013).
- ³⁹ P. Guyot-Sionnest, J. H. Hunt, and Y. R. Shen, *Phys. Rev. Lett.* **59**, 1597 (1987).
- ⁴⁰ E. Tyrode and J. Hedberg, *J. Phys. Chem. C* **116**, 1080 (2012).
- ⁴¹ J. C. Conboy, M. C. Messmer, and G. L. Richmond, *J. Phys. Chem. B* **101**, 6724 (1997).
- ⁴² A. M. Briggs, M. S. Johal, P. B. Davies, and D. J. Cooke, *Langmuir* **15**, 1817 (1999).